Optical Properties of PbS and Au-PbS Core-Shell Nanoparticles

Sai Cong Doanh, Pham Nguyen Hai, Ngac An Bang[*]

Faculty of Physics, VNU University of Science, 334 Nguyen Trai, Hanoi, Vietnam

Abstract: Lead sulfide (PbS) and Au-PbS core-shell nanoparticles were successfully synthesized using the sonochemical method at room temperature. The morphology of the synthesized particles was characterized by FESEM and TEM images. Pure fcc phase of PbS and Au crystal structures was examined and confirmed by XRD patterns. The quantum confinement effect plays a crucial role in blue-shifting the absorption edge and the band gap energy of both solid PbS nanoparticles and a thin spherical PbS shell toward shorter wavelength region in comparison to those of PbS bulk. Due to the high refractive index of PbS shell, Surface Plasmon Resonance (SPR) peak of Au nanocores is significantly red-shifted by roughly 80 nm toward the longer wavelength region. More sophisticate experimental data and some adequate theoretical models are needed to fully explain the matters.

Keywords: PbS nanoparticle, Au-PbS core-shell nanoparticle, quantum confinement, Surface Plasmon Resonance (SPR).

1. Introduction

Lead sulfide (PbS) is classified to be in a class of IV-VI semiconductors with a narrow direct band gap energy of 0.41 eV at 300 K [1]. Due to the strong quantum confinement effect, the band gap energy of PbS nanomaterils can be tuned in the near infrared and even in the visible regions leading them to be employed in a lot of applications such as IR detectors, glucose sensor [2, 3], photo-transitors [4], solar absorber [5] or materials for luminescent display device [6], recently. Furthermore, metal-semiconductor heterostructures such as Au-PbS, Au-Cu_2O, Ag-Cu_2O and Au-SnO_2 core-shell nanoparticles or TiO_2-Ag and ZnO-Au composites have been finding themselves in many applications since they can integrate several functionalities required in one single structure [7-12].

In this paper, PbS and Au-PbS core-shell nanoparticles were synthesized by sonochemical method [13]. The synthesized samples were then subjected to characterizations such as XRD, FESEM, TEM and optical absorption analysis. Quantum confinement effect of PbS nanostructures was under study. The dependence of the Surface Plasmon Resonance (SPR) of gold nanoparticles on the refractive index of the medium was also investigated.

---

[*] Corresponding author. Tel.: 84- 912197071.
Email: ngacanbang@hus.edu.vn

2. Experimental

Lead sulfide nanoparticles were synthesized using the sonochemical method [13]. Briefly, a mixed aqueous solution of lead acetate trihydrate $Pb(CH_3COO)_2.3H_2O$ ($Pb(Ac)_2$), thioacetamide CH_3CSNH_2 (TAA) and cetyltrimethyl ammonium bromide $C_{19}H_{42}BrN$ (CTAB) at a certain molar ratio was treated with ultrasonic irradiation for an hour at room temperature. The resulting precipitate was then centrifuged and washed with absolute ethanol five times to remove the surfactant and other possible residues.

Quasi-spherical gold nanoparticles were synthesized and then used as the core for the fabrication of Au-PbS core-shell nanoparticles. The synthesis procedure of the gold nanoparticles was reported in detail elsewhere [14]. The Au-PbS nanoparticles were fabricated using the same sonochemical method with sodium dodecyl sulfate $C_{12}H_{25}NaO_4S$ (SDS) being used as both surfactant and structure-directing agent instead of CTAB.

The crystal structure of the synthesized samples was characterized by a Siemens D5005 XRD diffractometer. The morphologies of the nanoparticles were observed by a Nova nanoSEM 450 and a FEI Tecnai $G^2$20 FEG (TEM). The absorption spectra of the samples were recorded at room temperature using a Shimadzu UV-Vis-2450PC and Carry 5000 spectrometer.

3. Results and discussion

Figure 1.a. shows a typical XRD pattern of the as-synthesized PbS samples and the standard card of the fcc phase of lead sulfide crystal structure (PDF 05-0667 ICDD). Several well-resolved diffraction peaks at 26.0^o, 30.1^o, 43.1^o, 51.0^o, 53.5^o and 63.6^o can readily be well-indexed to those of the (111), (200), (220), (311), (222) and (400) planes of the pure fcc phase of PbS (PDF 05-0667 ICDD). No other impurities were found and the lattice constant a was determined to be $a = 5.933 \pm 0.008 \overset{o}{A}$. A typical FESEM image of the as-synthesized PbS nanoparticles is shown in Fig.1.b. The PbS nanoparticles appear to be quasi-spherical in shape with a rough surface and their average size was estimated to be 41.6 nm with the standard deviation of 5.1 nm.

Optical properties of the synthesized PbS nanoparticles were investigated by using the absorption spectrum. As it can be seen in Fig. 1. c., the absorption spectrum of the synthesized PbS nanoparticles exhibits no absorption peak but a stiff absorption edge in the near-infrared region. Since PbS is a direct band gap semiconductor, the band gap energy E_g of synthesized PbS nanoparticles was determined from the plot of $(\alpha h\nu)^2$ as a function of the incident photon energy $h\nu$ with α being the absorption coefficient. A modified linear function $F(h\nu) = A(h\nu - E_g)$, where A is a constant, was fitted to the straight portion of the graph on the edge as shown in Fig.1.d. The band gap energy E_g was then determined to be 1.16 eV, which is much larger than the well-reported value of 0.41 eV for the bulk PbS [1, 13]. The observed blue-shift of the absorption edge and the band gap energy E_g of the synthesized PbS nanoparticles can be attributed to the quantum confinement effect of PbS nanoparticles. There are several theoretical models such as the effective mass model, hyperbolic band model, cluster model … which can be used to explain the dependence of the band gap energy on the size of PbS nanoparticle [15]. Unfortunately, all of those models fail in describing our experimental data. Beside the fact that the synthesized PbS nanoparticles have a rather broad size distribution, the size-dependent effect of the dielectric constant ε of PbS nanoparticle should also be taken into account in those mentioned theoretical models.
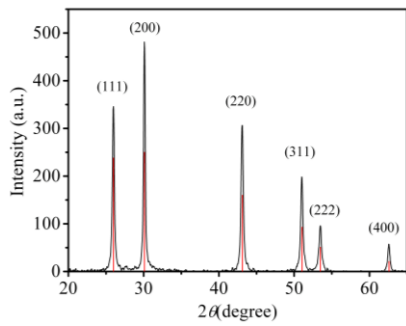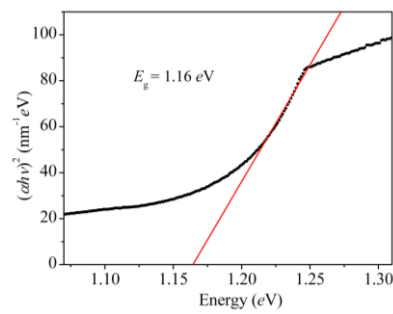
a. Typical XRD spectrum of PbS nanoparticles.
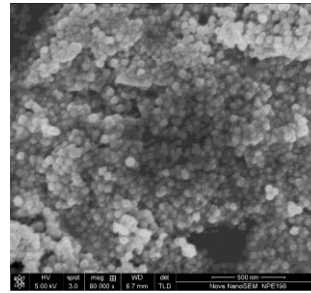
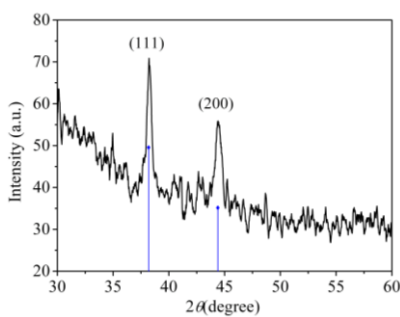

b. Typical TEM image of PbS nanoparticles.
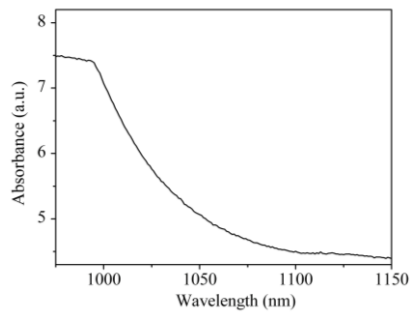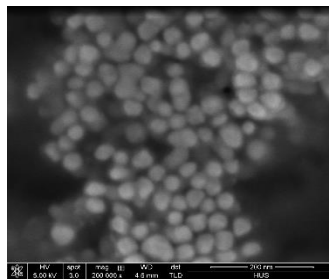

c. Absorption spectrum of PbS nanoparticles.

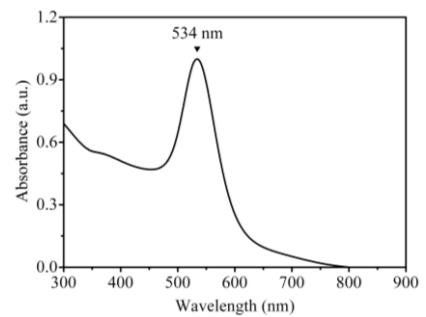d. Plot of $(\alpha h v)^2$ as a function of the incident photon energy hv.

Fig.1. The typical XRD patterns (a), TEM image (b), absorption spectrum (c) of the synthesized PbS nanoparticles and the plot of $(\alpha h v)^2$ as a function of the incident photon energy hv (d).

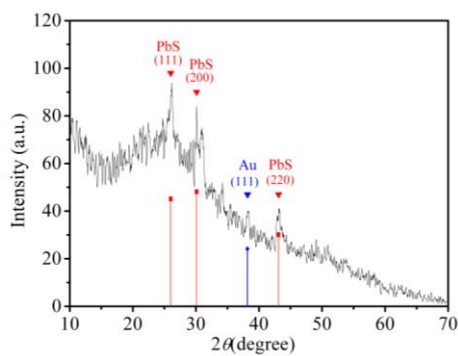a. Typical XRD pattern of the synthesized Au nanoparticles.

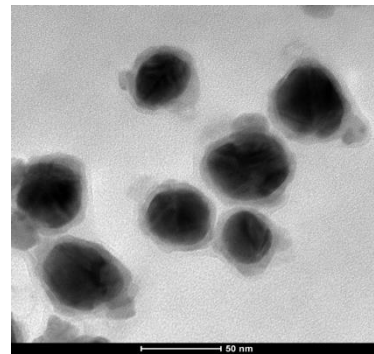b. Typical FESEM image of the synthesized Au nanoparticles.

c. Absorption spectrum of the synthesized Au nanoparticles.

Figure 2. The typical XRD pattern (a), FESEM image (b) and UV_vis spectrum (c) of the synthesized Au nanoparticles.

Figure 2.a shows a typical XRD pattern of the gold nanoparticles synthesized using the chemical reduction method and used as the core particles in preparation of Au-PbS core-shell nanoparticles. The pattern exhibits two well-resolved (111) and (200) diffraction peaks which could be well indexed to the faced-center cubic (fcc) phase of metallic gold structure (PDF 04-0784, ICDD). The lattice constant a was calculated to be $a = 4.077 \pm 0.002 \overset{\circ}{A}$. Figure 2.b. shows a typical FESEM image of the synthesized gold nanoparticles. Being quasi-spherical in shape, the average size of the Au nanoparticles was estimated to be 41.4 ± 4.7 nm. The UV_Vis spectrum of the synthesized Au nanoparticles is shown in Fig.2.c. As expected, the UV_Vis spectrum exhibits only one absorption peak at about 534 nm corresponding to the dipole Surface Plasmon Resonance (SPR) of the symmetric spherical gold nanoparticles [14, 16].
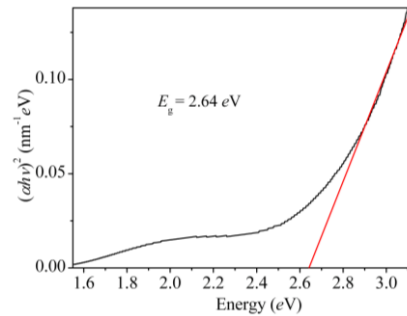

a. Typical XRD pattern of the synthesized Au-PbS core-shell nanoparticles.

b. Typical TEM image of the synthesized Au-PbS core-shell nanoparticles.
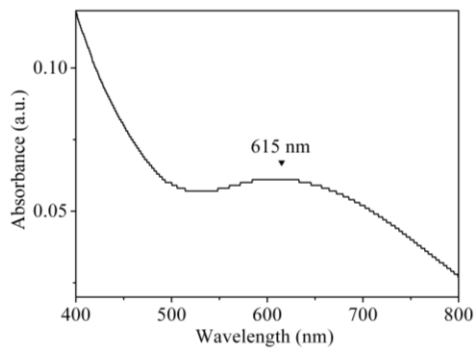
c. Absorption spectrum of the synthesized Au-PbS core-shell nanoparticles.

d. Plot of $(\alpha h v)^2$ as a function of the incident photon energy hv.

Figure 3. The typical XRD patterns (a), TEM image (b), absorption spectrum (c) of the synthesized Au-PbS core-shell nanoparticles and the plot of $(\alpha h v)^2$ as a function of the incident photon energy hv (d).

Crystal structure of the synthesized Au-PbS nanoparticles was again examined by using the XRD pattern. A typical XRD pattern of the synthesized Au-PbS nanoparticles is shown in Fig.3.a. As already described above, Au-PbS colloidal nanoparticles were synthesized and then suspended in ethanol at a very low concentration. Thus, there are only three clear, but rather weak, diffraction peaks at 26.0^{o}, 30.1^{o} and 43.1^{o}, which could be identified as those of the (111), (200) and (220) planes of the pure fcc phase of PbS (PDF 05-0667 ICDD), respectively. The pattern also exhibits a well-resolved diffraction peak at 38.2^{o} which could be well indexed to that of the (111) plane of the faced-center cubic (fcc) phase of metallic gold structure (PDF 04-0784, ICDD). The morphology of the synthesized Au-PbS nanoparticles was characterized using TEM images with the help of the image processing program ImageJ. A typical TEM images of the synthesized Au-PbS core-shell nanoparticles is shown in Fig.3.b., which clearly indicates the core-shell structure with only one Au core at the center and a thin PbS shell. No particle with multiple cores or without core was observed. Due to their similar crystal structure, it is possible that PbS could be nucleated and epitaxially grown on the surface of the Au core to form a rough shell of PbS covering the entire surface of gold particle. On average, the thickness of the PbS shell was estimated to be about 5.1 ± 1.1 nm.

The absorption spectrum of the Au-PbS core-shell nanoparticles is shown in Fig. 3.c. The absorption edge is significantly shifted toward shorter wavelength region in comparison to the case of the solid PbS nanoparticles discussed above. The band gap energy E_g of the synthesized Au-PbS core-shell nanoparticles was again determined from the plot determined from the plot of $(\alpha h v)^2$ as a function of the incident photon energy hv with α being the absorption coefficient as shown in Fig.3.d. The band gap energy E_g was then determined to be 2.64 eV, which is much larger than that of the solid PbS nanoparticles of 41.6 ± 5.1 nm in size. The observed blue-shift of the absorption edge and the band gap energy E_g of the PbS layer of about 5.1 nm in thickness are again due to the quantum confinement effect. Unlike the case of the solid PbS nanoparticle, there is no suitable theoretical model to explain the dependence of the band gap on the thickness of a thin spherical PbS shell.

The UV_vis spectrum of the Au-PbS core-shell nanoparticles shown in Fig. 3.c. also exhibits an absorption peak at about 615 nm which can be attributed to the SPR peak of quasi-spherical Au nanocores. In comparison to the SPR of Au nanocores suspended in water shown in Fig. 2.c, the SPR peak of the Au cores is significantly red-shifted from 534 nm to 615 nm. SPR of noble metallic nanoparticles depends not only on the shape and size of the particles but also on the refractive index of the medium in which they are embedded in [16]. In the case of the Au-PbS core-shell nanoparticles, the high refractive index of PbS shell (ranging from 3.6818 to 4.5975 in the visible region [17]) is responsible for the large red shift of the SPR peak of Au core. The broader SPR peak of the gold cores may indicate the variation of the thickness and uniformity of the PbS shell.

4. Conclusion

PbS and Au-PbS core-shell nanoparticles were successfully synthesized using the sonochemical method at room temperature. Due to the quantum confinement effect, the band gap energy of PbS solid nanoparticles of 41.6 ± 5.1 nm in size is significantly blue-shifted to 1.16 eV in comparison to that of the bulk PbS. For a thin spherical PbS shell of about 5.1 nm in thickness, the band gap energy is drastically shifted further to 2.64 eV. Current theoretical calculations appear to be not suitable to explain the obtained experimental data. More sophisticate experimental data and some adequate theoretical models are needed.

Surface Plasmon Resonance of Au nanoparticles depends strongly on the shape and the size of the particle as well as the refractive index of the medium. The SPR peak of Au nanoparticles of about 41

nm in size covered entirely by a thin spherical PbS shell of about 5.1 nm in thickness is significantly red-shifted by roughly 80 nm toward the longer wavelength region due to the high refractive index of PbS shell. Adequate theoretical calculation is required to fully explain the dependence of the SPR of noble metallic nanoparticles on the electrical properties of the surrounding medium.

References

[1] Kohn S E, Yu P Y, Petroff Y, Shen Y R, Tsang Y and Cohen M L 1973 Phys. Rev. B 8 1477.

[2] Xiaofei Liu, Mingde Zhang, International Journal of Infrared and Millimeter Waves, 2000, Volume 21, Issue 10, pp 1697–1701.

[3] Sai Cong Doanh, Luu Manh Quynh, VNU Journal of Science: Mathematics – Physics, Vol. 31, No. 2 (2015) 61-67.

[4] Zhenhua Sun, Jinhua Li and Feng Yan, J. Mater. Chem., 2012,22, 21673-21678

[5] V.M. García, M.T.S. Nair, P.K. Nair, Solar Energy Materials, Volume 23, Issue 1, November 1991, Pages 47-59

[6] Vanessa Wood and Vladimir Bulovic, Nano Reviews 2010, 1: 5202.

[7] Chun-Hong Kuo, Tzu-En Hua and Michael H. Huang, J. Am. Chem. Soc., 2009, 131 (49), pp 17871–17878.

[8] Jiangtian Li, Scott K. Cushing, Joeseph Bright, Fanke Meng, Tess R. Senty, Peng Zheng, Alan D. Bristow, and Nianqiang Wu, ACS Catal., 2013, 3 (1), pp 47–51.

[9] Jong-Soo Lee, Elena V. Shevchenko and Dmitri V. Talapin, J. Am. Chem. Soc., 2008, 130 (30), pp 9673–9675

[10] Kuai Yu , Zhengcui Wu , Qingrui Zhao , Benxia Li , and Yi Xie, J. Phys. Chem. C, 2008, 112 (7), pp 2244–2247.

[11] Tsutomu Hirakawa and Prashant V. Kamat, J. Am. Chem. Soc., 2005, 127 (11), pp 3928–3934.

[12] Jih-Jen Wu, Chan-Hao Tseng, Applied Catalysis B: Environmental, Volume 66, Issues 1–2, 2006, Pages 51–57.

[13] Le Van Vu, Sai Cong Doanh, Le Thi Nga, and Nguyen Ngoc Long, e-J. Surf. Sci. Nanotech. Vol. 9 (2011) 494-498.

[14] Ngac An Bang, Phung Thi Thom and Hoang Nam Nhat, 2013, Volume 46, Issue 2, pp 91–96.

[15] Y. Wang, A. Suna, W. Mahler, and R. Kasowski, J. Chem. Phys. 87, 7315 (1987).

[16] Perez-Juste J, Pastoriza-Santos I, Liz-Marzan LM, Mulvaney P, Coord Chem Rev (2005) 249:1870

[17] http://www.filmetrics.com/refractive-index-database/PbS/Lead-Sulfide